Desalination and Water Treatment
www.deswater.com
doi: 10.1080/19443994.2015.1043587

57 (2016) 10969–10979
May

Taylor & Francis
Taylor & Francis Group

Humic acid removal by electrocoagulation: characterization of aluminum species and humic acid

Ronna Jane S. Palacios, Do-Gun Kim, Seok-Oh Ko*

Department of Civil Engineering, Kyung Hee University, Yongin 446701, Korea, Tel. +82 31 201 2999; Fax: +82 31 202 8805; emails: rjpalacios@khu.ac.kr (R.J.S. Palacios), dogun.kim@khu.ac.kr (D.-G. Kim), soko@khu.ac.kr (S.-O. Ko)

Received 5 September 2014; Accepted 15 April 2015

ABSTRACT

In this study, the different aluminum (Al) species generated during electrocoagulation (EC), the humic acid (HA) removal, and the change in HA characteristics were evaluated. The results show that the distribution of monomeric Al species (Al_a), medium polymer Al species (Al_b), and colloidal or solid Al species (Al_c) was dependent on initial pH and current density (CD). The higher the fraction of Al_b and Al_c, the faster the HA removal. The fraction of Al_b and HA removal rates were higher at an initial pH of 4.5 than at 6.5. At a CD of 29 A m^{-2}, the fraction of Al_b and Al_c was higher and HA removal was faster than at 5 A m^{-2}. The results of UV/Vis spectroscopy, fluorescence spectroscopy, and size-exclusion chromatography show a decrease in aromaticity, degree of conjugation, and average molecular weight after EC treatment. The decreases were more pronounced at a high CD than at a low CD, indicating that Al_b and Al_c, especially Al_c, contribute much to the preferential removal of highly condensed and high molecular weight structures of HA by adsorption and patch coagulation.

Keywords: Electrocoagulation; Humic acid; Ferron analysis; Fluorescence; Molecular size distribution

1. Introduction

Natural organic matter (NOM) is present in natural aquatic systems and has caused problems in the water industry in terms of purification [1]. NOM can affect water treatment processes as it is a precursor of disinfection byproducts, can stimulate biological regrowth in water distribution systems, can lead to color, taste, or odor in waters and can cause organic fouling of membranes [2].

There are various NOM treatment technologies such as adsorption, oxidation, and coagulation. The use of different adsorbents, such as activated carbon [3], natural zeolite [4], biosorbents [5], and graphite oxide [6], has been proven to be effective, but these adsorbents are costly and the spent adsorbent needs to be disposed of after detoxification. Ozonation effectively transforms the hydrophobic part of NOM into hydrophilic reaction products [7]. Ozonation also reduces the aromaticity of NOM, leading to the formation of smaller size organic compounds with lower molecular weight. It can also increase the biodegradability of NOM [8,9]. However, undesirable byproducts such as aldehydes, organic acids, and aldo- and keto-acids can be generated after oxidation of NOM [10]. Coagulation has been proven to be an effective

*Corresponding author.

method of NOM removal [11]. However, a great volume of sludge is generated and the sludge requires further treatment [12].

Recently, electrocoagulation (EC) has been successfully tested for wastewater treatment. EC is a process where the coagulants are supplied by the electrodissolution of metal electrodes, instead of the addition of metal salts. Therefore, it is generally required to add background electrolyte to EC reactors [13]. In addition, separation of the flocs can be difficult because the O_2 and H_2 bubbles, produced by the electrolysis of water, can disturb settling and because an additional floatation device is necessary when the bubbles are not enough to float the flocs [13,14]. However, EC offers great advantages of high efficiency, fast reaction rates, versatility, simplicity, amenability to automation, cost-effectiveness, easy compact instrumentation, minimum use of chemicals, and ease of operation [13]. Previous studies have proven that EC is very efficient in NOM removal [5,14,15]. In addition, pH and current density (CD) play important roles in the removal of NOM by EC. However, the mechanisms of NOM removal by EC remain unclear. It seems that the mechanisms of pollutant removal by EC are similar to those by chemical coagulation (CC), i.e. charge neutralization precipitation. In CC, using Al salts, the formation of different Al species affects pollutant removal.

The hydrolysis Al species formed during the coagulation process can be classified into fast-reacting monomeric (Al_a), slow-reacting medium polymeric (Al_b), and nonreacting polymeric (Al_c) Al species based on the kinetic reactions between the aluminum and Ferron reagent [16,17]. According to Yan et al. [18], Al_a is mainly composed of monomeric species such as Al^{3+}, $Al(OH)^{2+}$, dimer ($Al_2(OH)_2^{4+}$), and trimer ($Al_3(OH)_4^{5+}$). Al_b is the intermediate polymer species formed during Al(III) hydrolysis, and Al_b content is correlated to the content of tridecamer ($Al_{13}O_4(OH)_{24}^{7+}$), often denoted as Al_{13} [19]. The colloidal or solid Al_c species is an inert large polymer or colloidal species formed during Al(III) hydrolysis, with a molecular weight normally larger than 3 kDa [18]. Al_a reacts with organic matter, forming aggregates to be removed. Al_b is superior to other species in charge neutralization, which could destabilize colloids and organic matter to form smaller flocs. In addition, Al_c can adsorb particles and organic matter to form larger flocs through patch coagulation [18].

The effects of Al species distribution on humic acid (HA) removal have been investigated for CC with Al salts [20,21]. When polyaluminum chloride sulfate (PACS) was used, the highest HA removal efficiency was achieved when the fraction of Al_c was the highest and that of Al_a and Al_b was the lowest at low Al doses (total Al < 0.15 mM) [21]. On the other hand, DOC and turbidity removal efficiency from eutrophic lake water were positively correlated to the amount of Al_b at pH > 6 when $AlCl_3$ or polyaluminum chloride (PACl) was used [20]. It is evident that Al speciation significantly affects organic pollutant removal efficiency by coagulation.

The distribution of Al species is controlled by pH and dosage of Al coagulant. In EC, the electric current and the oxidation–reduction reactions in the vicinity of the electrodes significantly affect the solution pH and the formation of Al species. Therefore, investigation of the relationships between Al species distribution and HA removal could provide valuable information about the mechanisms of HA removal by EC. In this study, the formation of Al species was explored and correlated to HA removal at different EC conditions. In addition, the changes in HA characteristics by EC were investigated using spectroscopic analysis and molecular weight distribution analysis.

2. Materials and methods

2.1. EC experiment

Al electrodes of 25 × 150 mm (thickness: 5 mm) were used for both anode and cathode, at a distance of 14 mm. The electrodes were scrubbed with sandpaper, soaked with 1% HCl, and rinsed with deionized water (DIW) several times to remove the passivation on the surface [13]. Batch EC experiments were carried out in a 1 L beaker. The electrodes were immersed into the solution in the beaker and the solution was agitated at 100 rpm with a mechanical stirrer. EC was applied immediately after starting agitation with a DC power supply (SI-30200A, CNG, Korea).

2.2. Al species determination and floc characterization

To investigate the Al species distribution during EC, batch experiments were conducted with Al electrodes and DIW containing 1 g L^{-1} NaCl as the background electrolyte [22]. The initial pH was 4.5 and 6.5 with a CD of 29 A m^{-2}, where the final pH was 6.8 and 7.8, respectively, and the CD was 5 and 29 A m^{-2} at an initial pH of 6.5, where the final pH was 6.9 and 7.8, respectively. The initial pH was adjusted using 1 M NaOH or HCl. Aliquots were taken periodically to analyze the Al species distribution.

The Ferron method was used to analyze the distribution of Al_a, Al_b, and Al_c species in the flocs [5] generated during EC in the absence of HA. Reagent A (0.2%, w/v, Ferron) was prepared by dissolving 2 g

Ferron (8-hydroxy-7-iodoquinoline-5-sulfonic acid, Sigma Chem. Co., USA) in 1 L preboiled and cooled DIW. Reagent B (20%, w/v, sodium acetate) was prepared by dissolving 200 g sodium acetate in 1 L DIW. Reagent C (1:9, v/v, HCl) was prepared by mixing 100 mL hydrochloric acid (37%) into 900 mL DIW. All reagents were filtered with a 0.45 μm PVDF filter before use. The Ferron colorimetric solution was obtained by mixing reagent B and C prior to the addition of reagent A. The volume ratio of the reagents A, B, and C was 2.5:2:1. The Ferron reagent was kept in a refrigerator and used within 3 weeks [23]. A 5 mL Al suspension was diluted with 14.5 mL DIW, and then 5.5 mL of Ferron reagent was added and shaken for homogeneity. The content of Al_a was measured by the absorbance at 366 nm using a UV/Vis spectrophotometer (UV mini 1240, Shimadzu) after 1 min of reaction, while that of $Al_a + Al_b$ was measured by the absorbance at 366 nm after 120 min. The total Al content (Al_T) was measured by inductively coupled plasma (OPTIMA 5300 DV, Perkin–Elmer, USA). The content of Al_c was obtained by the difference between the content of $Al_a + Al_b$ and that of Al_T.

Floc size distribution was analyzed for the flocs generated at 10 mg C L^{-1} HA, 5 A m^{-2} and at an initial pH of 6.5. The samples were collected periodically and were carefully handled to avoid the breaking up of macro flocs. The size of the flocs was monitored with an optical microscope (Optimus BX43, Japan). The floc size distribution was obtained with the aid of an image analysis technique, ImageJ, which is a public domain image processing tool developed by the National Institutes of Health (http://rsbweb.nih.gov/ij/). The zeta potential of the flocs was measured with a zeta potential analyzer (ZetaPlus, Brookhaven, USA) for the flocs obtained during EC at an initial pH of 4.5 or 6.5, either in the presence or absence of 10 mg C L^{-1} HA.

2.3. HA removal experiments

HA was obtained from the Aldrich Co. and purified according to Jee et al. [24]. The purified Aldrich HA (PAHA) stock solution was prepared by dissolving 1 g PAHA in 1 mL DIW and filtering with a 0.45 μm PVDF filter. The effects of initial pH were investigated at a pH range of 4.5–7.5 at 5 A m^{-2}, while those of CD were investigated at 5 and 29 A m^{-2}, at an initial pH of 6.5. The initial HA concentration was 10 mg C L^{-1}. Samples were taken periodically and filtered through 0.45 μm PVDF filters. HA concentration of the filtrates was measured using a TOC analyzer (TOC-V_{CPH}, Shimadzu, Japan).

2.4. HA characterization

The characteristics of HA during EC were investigated for the samples taken during EC at an initial pH of 6.5, at a CD of 5 and 29 A m^{-2} and at an initial HA concentration of 36.7 mg C L^{-1}. The initial HA concentration was higher than that for HA removal experiments (10 mg C L^{-1}), because the residual HA concentration was too low for proper characterization when the initial HA concentration was 10 mg C L^{-1}. The samples were filtered through a 0.45 μm PVDF filter. The filtrates were analyzed with a dual-beam UV/Vis spectrophotometer (UV mini 1240, Shimadzu, Japan) at wavelengths from 800 to 200 nm. The excitation–emission matrix (EEM) was generated by scanning excitation wavelengths from 240 to 400 nm with 5 nm increases, and detecting emission between 300 and 600 nm at 1 nm steps with a spectrofluorometer (RF5301PC, Shimadzu, Japan). Synchronous fluorescence (SF) spectra were also collected with constant offsets of 21, 32, 44, 55, 66, and 77 nm between excitation and emission wavelengths. The excitation wavelengths in the SF spectra were increased from 240 to 700 nm. The EEM and SF spectra of 1.0 mg C L^{-1} HA were obtained in the presence and in the absence of dissolved Al to identify the effects of dissolved Al on the EEM and SF spectrum of HA. The concentration of Al^{3+} from $AlSO_4$ was 1.0 mg L^{-1}, because it was found in a separate experiment that the maximum dissolved Al^{3+} concentration was 0.27 mg L^{-1} during 60 min of EC, when CD was 29 A m^{-2} and the initial pH was 6.5. The results showed that the EEM or SF spectrum of HA was not affected by the presence of dissolved Al (data not shown).

Molecular size distribution of HA was analyzed using size exclusion chromatography by an absorbance detector (UV 730 D, Younglin, Korea) and a Waters Protein Pak 125 column. The pH of the mobile phase was maintained at 6.8 by adding phosphate buffers (0.002 M $NaH_2PO_4 \cdot H_2O$ and 0.002 M Na_2HPO_4) to 0.1 M NaCl solution, and the flow rate was 0.8 mL min^{-1}. Four sodium polystyrene sulfonate (PSS) samples with actual apparent weight average molecular weights (MW_w) of 15.200, 6.530, 4.950, and 1.430 kDa (Polysciences, Inc., USA) and acetone (58 Da, HPLC grade, Aldrich, USA) were used as standards. All standards and samples were measured at a detection wavelength of 254 nm.

3. Results and discussion

3.1. Al species and size distribution of EC flocs

Fig. 1 presents the Al concentration obtained from the EC system at 1 g L^{-1} NaCl and the theoretical Al concentration calculated based on Faraday's law as in (Eq. (1)):

$$m = \frac{ItM}{zF} \tag{1}$$

where I is current (C s^{-1}), t is time (s), M is the molar mass of Al (g mol^{-1}), z is the valence of the dissolved metal in solution (equivalents per mole), and F is Faraday's constant (96,485 C mol^{-1}). Al concentration obtained from the experiments was higher than the theoretical value calculated from Faraday's law. This may be attributed to the dissolution of the cathode due to corrosion, in addition to the dissolution of the anode [25]. Mouedhen et al. [26] described the origin of excess dissolution as a chemical attack due to the acidity and alkalinity in the vicinity of the electrodes as follows:

In the vicinity of the anode:

$$2Al + 6H^+ \rightleftarrows 2Al^{3+} + 3H_2 \tag{2}$$

In the vicinity of the cathode:

$$2Al + 6H_2 + 2OH^- \rightleftarrows 2\left[Al(OH)_4\right]^- + 3H_2 \tag{3}$$

$$Al(OH)_3 + OH^- \rightleftarrows [Al(OH)_4]^- \tag{4}$$

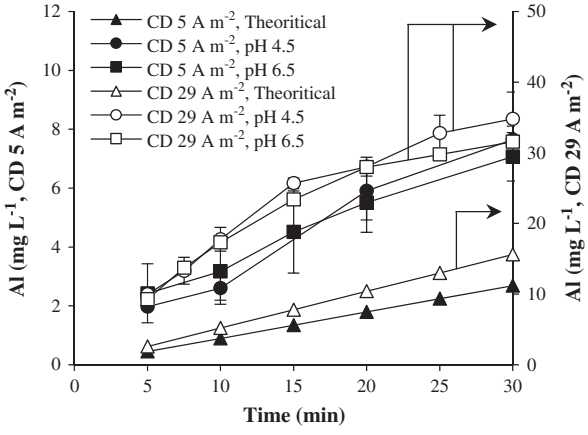

Fig. 1. Experimental vs. theoretical Al generation during EC (NaCl: 1 g L^{-1}).

As shown in Fig. 1, Al concentration increased as CD increased from 5 to 29 A m^{-2}. It seems that initial pH did not affect the Al dissolution. It is reported that the rate of Al dissolution and metal hydroxide formation on an electrode is not significantly different at an initial pH of 4.5–6.5 [27].

Fig. 2 shows the distribution of Al species during EC at different initial pHs and CDs. Regardless of initial pH and CD, Al_a was dominant and Al_b and Al_c increased as reaction time increased as shown in Fig. 2(a) and (b). At the same CD of 29 A m^{-2}, initial pH did not affect the fraction of Al_a, while the fraction of Al_b was slightly higher at pH 4.5. However, the fraction of Al_c was notably higher at initial pH 6.5 than 4.5 (Fig. 2(a)), indicating more Al_b transformed into Al_c at pH 6.5 than at pH 4.5. It has also been reported that the fraction of Al_c increases as pH increases [20]. Meanwhile, the total Al concentration during EC was not significantly dependent on initial pH (data not shown). Fig. 2(b) shows that CD affects the Al concentration and species distribution more significantly than initial pH. The decrease in Al_a and the

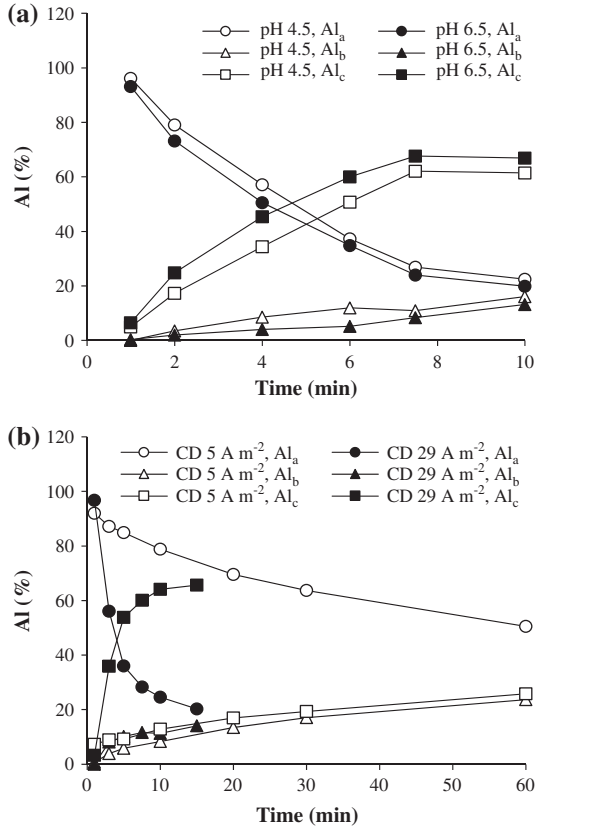

Fig. 2. Al species distribution (a) at different initial pHs at a CD of 29 A m^{-2} and (b) at different CDs at an initial pH of 6.5 (NaCl: 1 g L^{-1}).

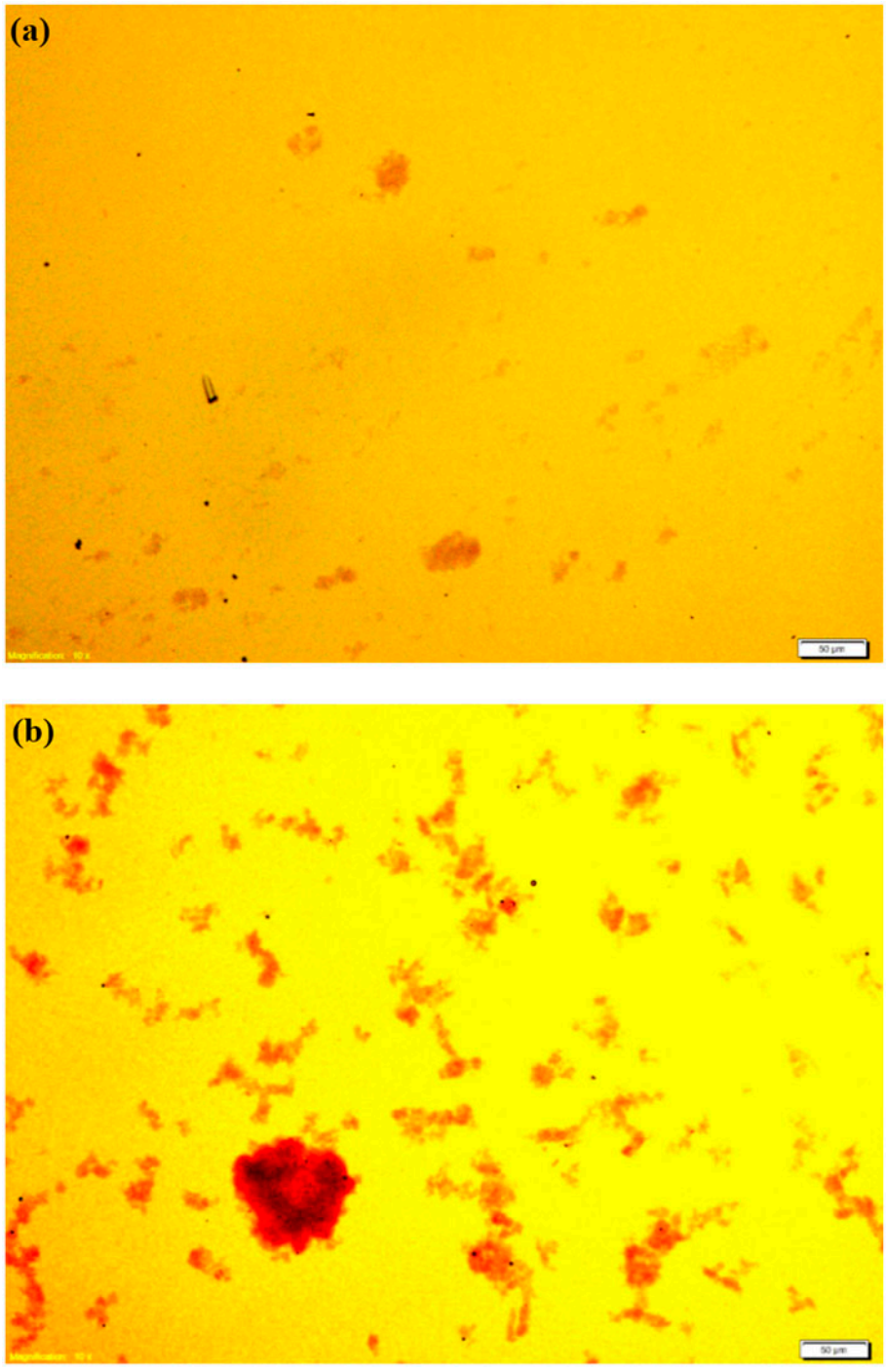

Fig. 3. Micrographs of the Al flocs formed during EC after (a) 17.5 and (b) 30 min (initial HA: 10 mg C L^{-1}, initial pH: 6.5, CD: 5 A m^{-2}, NaCl: 1 g L^{-1}).

increase in Al_c were a lot more dramatic at 29 A m^{-2} than at 5 A m^{-2}. It is regarded that the rapid increase in Al_c at high CD is due to the rapid increase in pH, via the OH^- generation at the cathode during electrolysis and coagulant amount. In addition, more colloidal or solid Al_c is formed at a high coagulant dose similar to sweep coagulation [13,20].

Fig. 3 provides images of EC flocs and the floc size distribution as a function of reaction time, when the initial HA was 10 mg C L^{-1}, initial pH was 6.5 and

CD was 5 A m^{-2}. No floc was observed during the first 15 min of the reaction, likely because of the high Al_a fraction. As expected, floc size increased as the reaction progressed from 17.5 to 30 min, due to the formation of Al_b and Al_c species. The mean diameter of the flocs at 17.5, 20, 25, and 30 min was 10.15 ± 6.94, 24.74 ± 11.74, 26.67 ± 12.81, and 30.01 ± 19.68 μm, respectively. The rapid increase in floc size during minutes 17.5–20 is thought to be due to the collision of the flocs. Spicer et al. [28] suggested that aggregates collisions produce larger irregular flocs until a steady state is reached.

3.2. HA removal by EC

3.2.1. Effect of pH

It has been reported that pH has a significant effect on the efficiency of the EC process in the removal of a variety of pollutants [5], because pH affects the surface charge of the flocs and the Al species distribution. Fig. 4(a) shows that the HA removal rate increased as the initial pH decreased, although the total Al concentration was similar regardless of pH. It is thought that the increase in HA removal at low pH is attributed to the enhanced charge neutralization by Al_b, which is generated more at low pH than at high pH (Fig. 2(b)). In addition, it is also thought that the results can be partly attributed to the HA characteristics at different pHs. When the pH value is low, acidic functional groups, i.e. carboxyl and phenol, of HA exist in the chemical form of –COOH and –OH. When pH is increased, they become deprotonated and exist in the form of $–COO^-$ and $–O^-$, which gives them a more negative charge [29]. This means that more positively charged Al^{3+} is necessary to neutralize the negatively charged HA [5]. The values of the pK_a's of the ionizable sites in carboxylic groups in Aldrich HA were reported to be 3.29 ± 0.03, 5.01 ± 0.04, and 6.38 ± 0.02, while those in phenolic groups were reported to be 7.95 ± 0.07 and 9.41 ± 0.06, at 1.0 mol L^{-1} NaCl [30]. Also, the values of pK_a's of gray HA was also

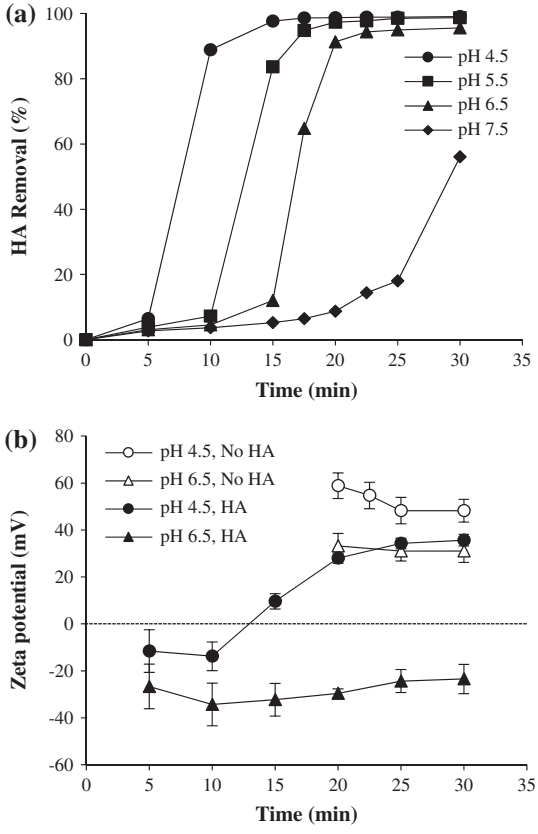

Fig. 4. Influence of initial pH on (a) HA removal and (b) zeta potential (initial HA: 10 mg C L^{-1}, CD: 5 A m^{-2}, electrode area: 40 cm^2, NaCl: 1 g L^{-1}).

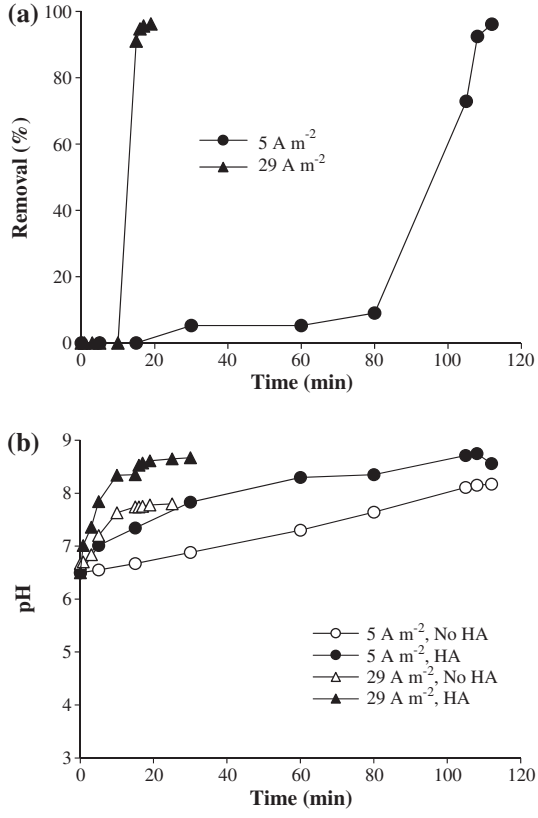

Fig. 5. (a) The effect of CD on HA removal efficiency with reaction time and (b) the effect of CD on pH during EC (initial pH: 6.5, initial HA: 10 mg C L^{-1}, NaCl: 1 g L^{-1}).

reported to be 3.99 and 8.05 [29]. Meanwhile, the final pH was 5.95, 6.72, 7.32, and 7.83 when the initial pH was 4.5, 5.5, 6.5, and 7.5, respectively.

In addition, the fraction of Al_b, the positively charged intermediate polymer Al species, was higher at pH 4.5 than pH 6.5 (Fig. 2(a)), indicating that more positively charged Al flocs are provided at a lower pH. This is partly supported by the results in Fig. 4(b), which suggest that the zeta potential of the flocs formed at the initial pH of 4.5 was more positive than at 6.5, regardless of the presence of HA. Fig. 4(b) also shows that the flocs formed in the presence of HA were more negatively charged than the flocs formed in the absence of HA, regardless of initial pH. This indicates the adsorption of negatively charged HA onto the flocs. It also indicates that charge neutralization significantly affects the HA removal rate of EC.

On the other hand, visible flocs began to form faster in the presence of HA than in the absence of HA. At the initial pH of 6.5, flocs were observed after 5 min in the presence of HA, while they were observed after 17.5 min in the absence of HA. It is thought that the early floc formation is attributed to the binding of Al species with HA. HA can form complexes with Al^{3+} or $AlOH^{2+}$, which is the dominant form of Al [31]. They correspond to Al_a, which is dominant at the early stage of EC (Fig. 2).

3.2.2. Effect of CD

As shown in Fig. 5(a), HA removal was a lot faster at 29 A m^{-2} than at 5 A m^{-2}. Fast removal at a high CD can be related to the higher fraction of Al_b and Al_c, as presented in Fig. 2(b). In particular, Al_c was significantly higher at high CD than at low CD. High Al_c content can lead to turbidity and organics removal via adsorption and electrostatic patch coagulation [18]. The floc size can also be increased by the coagulation induced by the local contact between the part ("patches") of the surface neutralized by adsorbing oppositely charged ions [32]. This improves pollutant removal efficiency by sweep flocculation [18]. The results from Fig. 5(a) strongly indicate that the distribution of Al species significantly affects HA removal. This result was additionally supported by the finding that a similar HA removal efficiency was achieved with a lower Al_t at 29 A m^{-2} than at 5 A m^{-2} (Fig. S1 in supporting information).

Fig. 5(b) shows that the pH during EC was higher in the presence of HA than in the absence of HA. This is attributed to the adsorption of organic acids to the flocs. The COO^- groups of the organic acid can replace the surface OH on oxides and the OH ions are released, resulting in the increase in pH [33].

3.3. HA characterization

3.3.1. SUVA

Variations in DOC and SUVA during EC are presented in Fig. 6. DOC and SUVA decreased during EC, both at 5 and 29 A m^{-2}. The decrease in SUVA indicates that the average molecular weight and aromaticity decreased in residual HA, as a result of the removal of more aromatic and high molecular weight fractions of HA [34]. It also indicates that the hydrophobicity of the HA decreased. Karanfil et al. [35] suggested that natural waters with high SUVA values, i.e. ≥0.04 L mg^{-1} cm^{-1}, have a relatively high content of hydrophobic, aromatic, and high molecular weight NOM fractions, whereas waters with SUVA values of ≤0.03 L mg^{-1} cm^{-1} contain largely nonhumic, hydrophilic, and low molecular weight materials. The SUVA of HA was 0.10 L mg^{-1} cm^{-1}, while it decreased to 0.0273 and 0.0189 L mg^{-1} cm^{-1} at 5 A m^{-2} (80 min) and 29 A m^{-2} (14 min), respectively.

The decrease in DOC and SUVA was faster at high CD. In addition, it was observed that the decrease in DOC and SUVA was greater at high CD at the same

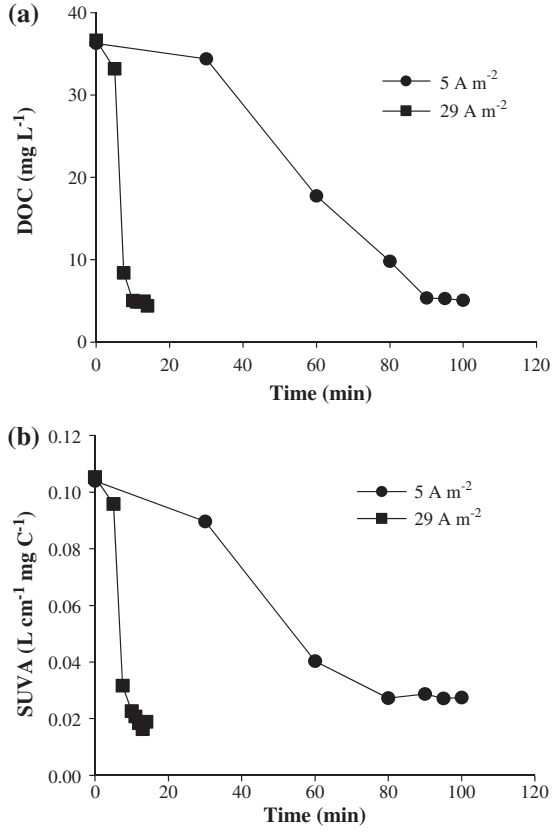

Fig. 6. The variation of (a) DOC and (b) SUVA with reaction time at different CDs (initial pH: 6.5, initial HA: 36.7 mg C L^{-1}, NaCl: 1 g L^{-1}).

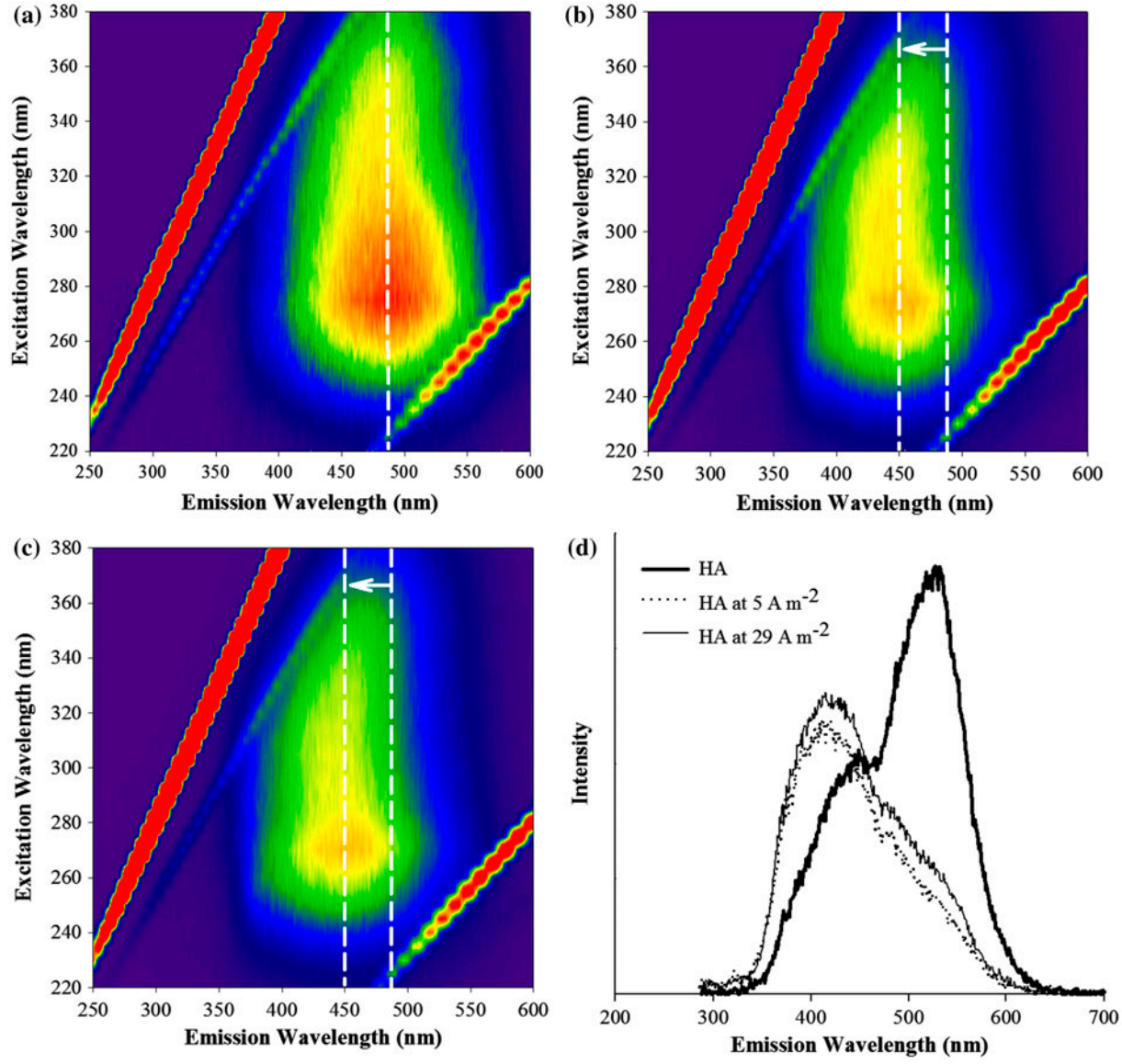

Fig. 7. Excitation–emission maps of (a) untreated HA, (b) the filtrate of HA treated using EC at a CD of 5 A m^{-2}, (c) the filtrate of HA treated using EC at a CD of 29 A m^{-2}, and (d) synchronous fluorescence spectra of HA and the filtrates of HA treated using EC (1 mg C L^{-1}, NaCl: 1 g L^{-1}).

Al_t (Fig. S2 in supporting information). Based on the Al species analysis shown in Fig. 2(a), it is thought that the greater decrease in SUVA is attributed to the relative abundance of Al_b and Al_c at high CD. Therefore, it is suggested that the medium polymer and/or colloidal Al (Al_b and Al_c) are more effective in the removal of high molecular weight and more conjugated HA fractions.

3.3.2. Fluorescence spectroscopy

The samples for fluorescence spectroscopic analysis and molecular weight analysis were taken at 50 and 6.5 min of reaction at 5 and 29 A m^{-2}, respectively. The HA concentration was 23.1 and 18.5 mg C L^{-1}, respectively. The pH of the samples was adjusted to 6.0 and the samples were diluted to 1 mg C L^{-1} for fluorescence spectroscopic analysis. Fig. 7(a) shows the characteristic peak of HA around Ex/Em 280/490 nm for untreated HA. The fluorophore at Ex/Em 250–260/380–420 nm corresponds to HA [34,36,37]. After EC, the intensity of the fluorophore decreased and the fluorophore shifted to a shorter emission wavelength, regardless of CD (Fig. 7(a) and (b)). The "blue shift" also appeared in SF spectra (Fig. 7(d)).

The position, shift, and intensity of fluorophore can be correlated to the structural information of NOM such as polycondensation, aromaticity, and the content of functional groups [38]. The decrease in the intensity of HA-characteristic fluorophore is attributed to the removal of carboxylic functional groups and aromatic structures [39]. The "blue shift" indicates the transformation of condensed aromatic moieties to smaller molecules, the reduction in the degree of π-electron systems such as decreasing the number of aromatic rings or conjugated bonds in a chain structure and the elimination of functional groups such as carbonyl, hydroxyl, and amine [39]. This is often observed as a result of the oxidation of humic substances [40,41], suggesting a potential mechanism for HA molecules with higher molecular weight and with a higher degree of aromaticity to be preferentially removed during EC.

3.3.3. Molecular weight distribution of HA

The molecular size distributions of HA, untreated and treated by EC, are provided in Fig. 8. Fig. 8 shows that molecules >1 kDa decreased and molecules <1 kDa increased after EC. The decrease in >1 kDa fractions and the increase in <0.5 kDa fractions were more significant at a high CD than at a low CD. The weight average molecular weight (MW_w), the number average molecular weight (MW_n), and polydispersity of HA were 985.40, 900.95, and 3.27 Da, respectively. They decreased to 729.39, 282.31, and 2.58 Da, respectively at a CD of 5 A m^{-2}, and continued to decrease at a high CD of 29 A m^{-2}, to 603.50, 240.96, and 2.50 Da, respectively. The decrease in MW_w and MW_n indicates the removal of more condensed large molecular weight fractions of HA, which is in agreement with the results of UV/Vis spectroscopy and fluorescence spectroscopy. The decrease in polydiversity indicates a decrease in heterogeneity of HA due to the preferential removal of large molecular weight fractions of HA. Meanwhile, the more significant decrease in average molecular weight at a high CD suggests that Al_b and Al_c are effective in the removal of high molecular weight fractions of HA.

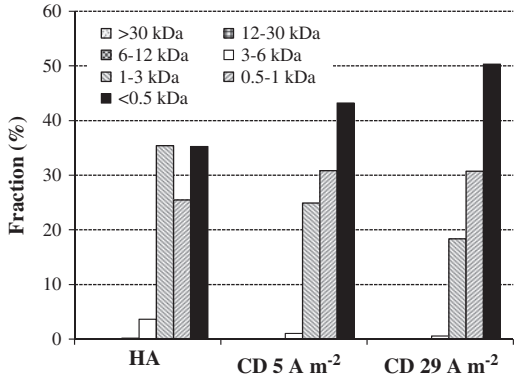

Fig. 8. Molecular weight distribution of HA and EC-treated HA (initial pH: 6.5, initial HA: 36.7 mg C L^{-1}, NaCl: 1 g L^{-1}, reaction time was 50 and 7 min for CD of 5 and 29 A m^{-2}, respectively).

Meanwhile, partial oxidation of HA by HOCl in the vicinity of anode might partly be responsible for the changes in SUVA254, fluorescence intensity and MW distribution provided in Figs. 6(b)–8. The chloride ions can be oxidized to form active chlorine species, such as chlorine, hypochlorous acid, and hypochlorite, on anode surface and in the bulk solution (Eqs. (5)–(7)) [42]. The active chlorine species can improve the oxidation of organic compounds.

$$2Cl^- \rightleftarrows Cl_2 + 2e^- \quad (5)$$

$$Cl_2 + H_2O \rightleftarrows HOCl + H^+ + Cl^- \quad (6)$$

$$HOCl \rightleftarrows H^+ + OCl^- \quad (7)$$

The pH of the bulk solution during the EC was higher than 6.5 where OCl^- is the dominant active Cl species. However, H^+ is generated from anode and there can be a layer with low pH, i.e. lower than 6.5 where HOCl is dominant, near the anode [43]. Therefore, the oxidation of HA can be more active on this layer than in bulk solution, because HOCl is more reactive than OCl^-.

It has been known that NOM molecules are partially oxidized by O_3 or H_2O_2 to lower molecular weight, higher polarity, and less condensed moieties, rather than to complete oxidation products [44]. It was reported that the oxidation of effluent organic matter with O_3 resulted in the decrease in UV254 and fluorescence intensity without a significant decrease in DOC [45]. Zhang et al. [46] also confirmed that NOM concentration was decreased after chlorination. In addition, the partial oxidation products of NOM are known to be aldehydes and carboxylic acids [47], which are the electron-withdrawing groups, reducing the fluorescence intensity [48].

4. Conclusions

In this study, HA removal mechanisms by EC using Al electrodes were investigated based on the generated Al species distribution and HA characteristics. During

EC, monomer Al_a was generated initially and transformed to medium polymer Al_b, then finally the colloidal or solid Al_c was formed. The distribution of Al_a, Al_b, and Al_c was highly affected by initial pH and CD. The fraction of Al_b was higher at an initial pH of 4.5, while that of Al_c was higher at 6.5. The fractions of Al_b and Al_c were much higher at a CD of 29 A m^{-2} than of 5 A m^{-2}. In addition, the floc size increased as reaction time and Al_c increased. The HA removal rate increased as the initial pH decreased, indicating that Al_b contributes much to HA. HA removal was faster at 29 A m^{-2} than at 5 A m^{-2}, in addition, the required Al amount for similar HA removal was less at 29 A m^{-2} than at 5 A m^{-2}. The results indicate that Al_b and Al_c play a dominant role in HA removal and that the predominant HA removal mechanism was adsorption and patch coagulation or bridging.

The EC-treated HA showed a decrease in SUVA, the "blue shift" of fluorophore, and a decrease in average molecular weight and polydispersity, indicating the preferential removal of highly conjugated, hydrophobic, high molecular weight fractions and carboxylic functional groups of HA by EC. In addition, the decrease in SUVA, average molecular weight and polydispersity was more significant at a high CD, evidencing that Al_c contributes much to the removal of high molecular weight fractions of HA.

Supplementary material

The supplemental material for this paper is available at http://dx.doi.org/10.1080/19443994.2015.1043587.

Acknowledgements

This subject is partially supported by Korea Ministry of Environment as "Converging technology project". This work was partially supported by the National Research Foundation of Korea (NRF) grant funded by the Korean government (MEST) (No. 2013R1A2A2A03016095).

References

[1] A. Matilainen, N. Lindqvist, S. Korhonen, T. Tuhkanen, Removal of NOM in the different stages of the water treatment process, Environ. Int. 28 (2002) 457–465.
[2] C. Park, H. Kim, S. Hong, S. Lee, S.I. Choi, Evaluation of organic matter fouling potential by membrane fouling index, Water Sci. Technol. 7 (2007) 27–33.
[3] S.B. Wang, Q. Ma, Z.H. Zhu, Characteristics of unburned carbons and their application for humic acid removal from water, Fuel Process Technol. 90 (2009) 375–380.
[4] S. Wang, W. Gong, X. Liu, B. Gao, Q. Yue, Removal of fulvic acids using the surfactant modified zeolite in a fixed-bed reactor, Sep. Purif. Technol. 51 (2006) 367–373.
[5] Q. Feng, X. Li, Y. Cheng, L. Meng, Q. Meng, Removal of humic acid from groundwater by electrocoagulation, J. China Uni. Mining Technol. 17 (2007) 513–515.
[6] T. Hartono, S.B. Wang, Q. Ma, Z. Zhu, Layer structured graphite oxide as a novel adsorbent for humic acid removal from aqueous solution, J. Colloid Interf. Sci. 333 (2009) 114–119.
[7] K.-C. Chen, Y.-H. Wang, Control of disinfection by-product formation using ozone-based advanced oxidation processes, Environ. Technol. 33 (2012) 487–495.
[8] H. Zhu, X.H. Wen, X. Huang, Pre-ozonation for dead-end microfiltration of the secondary effluent: Suspended particles and membrane fouling, Desalination 231 (2008) 166–174.
[9] H. Zhu, X.H. Wen, X. Huang, Membrane organic fouling and the effect of pre-ozonation in microfiltration of secondary effluent organic matter, J. Membr. Sci. 352 (2010) 213–221.
[10] P.C. Singer, Formation and characterization of disinfection byproducts, in: G.F. Craun, Safety of Water Disinfection: Balancing Chemical & Microbial Risks, ILSI Press, Washington, DC, 1993, pp. 201–220.
[11] E.S. Rigobello, A. Di Bernardo Dantas, L. Di Bernardo, E.M. Vieira, Influence of the apparent molecular size of aquatic humic substances on colour removal by coagulation and filtration, Environ. Technol. 32 (2011) 1767–1777.
[12] S. Malhotra, Polyaluminium chloride as an alternative coagulant, Affordable Water Supply and Sanitation, Proceedings of the 20th WEDC Conference, Colombo, Sri Lanka, 1994.
[13] B. Al Aji, Y. Yavuz, A.S. Koparal, Electrocoagulation of heavy metals containing model wastewater using monopolar iron electrodes, Sep. Purif. Technol. 86 (2012) 248–254.
[14] A.S. Koparal, Y.S. Yildiz, B. Keskinler, N. Demircioğlu, Effect of initial pH on the removal of humic substances from wastewater by electrocoagulation, Sep. Purif. Technol. 59 (2008) 175–182.
[15] D. Ghernaout, B. Ghernaout, A. Saiba, A. Boucherit, A. Kellil, Removal of humic acids by continuous electromagnetic treatment followed by electrocoagulation in batch using aluminium electrodes, Desalination 239 (2009) 295–308.
[16] R.W. Smith, Nonequilibrium systems in natural water chemistry, in: J.D. Hem, Advances in Chemistry, vol. 106, American Chemical Society, Washington, DC, 1971, pp. 117–168.
[17] P.M. Jardine, L.W. Zelazny, Mononuclear and polynuclear aluminum speciation through differential kinetic reactions with ferron, Soil Sci. Soc. AM. J. 50 (1986) 895–900.
[18] M. Yan, D. Wang, J. Qu, W. He, C.W.K. Chow, Relative importance of hydrolyzed Al(III) species (Al_a, Al_b, and Al_c) during coagulation with polyaluminum chloride: A case study with the typical micro-polluted source waters, J. Colloid Interface Sci. 316 (2007) 482–489.

[19] P.M. Bertsch, Aqueous polynuclear aluminum species, in: G. Sposite, The Environmental Chemistry of Aluminium, Boca Raton, CRC Press, 1989, pp. 250–279.
[20] C. Hu, H. Liu, J. Qu, D. Wang, J. Ru, Coagulation behavior of aluminum salts in eutrophic water: Significance of Al^{13} species and pH control, Environ. Sci. Technol. 40 (2006) 325–331.
[21] Z. Wu, P. Zhang, G. Zeng, M. Zhang, J. Jiang, Humic acid removal from water with polyaluminum coagulants: Effect of sulfate on aluminum polymerization, J. Environ. Eng. ASCE 138 (2012) 293–298.
[22] A.K. Golder, A.N. Samanta, S. Ray, Removal of trivalent chromium by electrocoagulation, Sep. Purif. Technol. 53 (2007) 33–41.
[23] W. Zhou, B. Gao, Q. Yue, L. Liu, Y. Wang, Al–Ferron kinetics and quantitative calculation of Al(III) species in polyaluminum chloride coagulants, Colloid Surf. A. 278 (2006) 235–240.
[24] S.H. Jee, Y.J. Kim, S.O. Ko, Transformation of dissolved organic matter by oxidative polymerization with horseradish peroxidase, Water Sci. Technol. 62 (2010) 340–346.
[25] K. Mansouri, A. Hannachi, A. Abdel-Wahab, N. Bensalah, Electrochemically dissolved aluminum coagulants for the removal of natural organic matter from synthetic and real industrial wastewaters, Ind. Eng. Chem. Res. 51 (2012) 2428–2437.
[26] G. Mouedhen, M. Feki, M. Wery, Behavior of aluminum electrodes in electrocoagulation process, J. Hazard. Mater. 150 (2008) 124–135.
[27] C.P. Nanseu-Njiki, S.R. Tchamango, P.C. Ngom, A. Darchen, E. Ngameni, Mercury(II) removal from water by electrocoagulation using aluminium and iron electrodes, J. Hazard. Mater. 168 (2009) 1430–1436.
[28] P.T. Spicer, W. Keller, S.E. Pratsinis, The effect of impeller type on floc size and structure during shear-induced flocculation, J. Colloid Interface Sci. 184 (1996) 112–122.
[29] R.A. Alvarez-Puebla, J.J. Garrido, Effect of pH on the aggregation of a gray humic acid in colloidal and solid states, Chemosphere 59 (2009) 659–667.
[30] J.C. Masini, G. Abate, E.C. Lima, L.C. Hahn, M.S. Nakamura, J. Lichtig, H.R. Nagatomy, Comparison of methodologies for determination of carboxylic and phenolic groups in humic acids, Anal. Chim. Acta. 364 (1998) 223–233.
[31] E. Tipping, C. Rey-Castro, S.E. Bryan, J. Hamilton-Taylor, Al(III) and Fe(III) binding by humic substances in freshwaters, and implications for trace metal speciation, Geochim. Cosmochim. Acta 66 (2002) 3211–3224.
[32] Y-L. Cheng, R-J. Wong, J.C-T. Lin, C. Huang, D-J. Lee, A.S. Mujumdar, Water coagulation using electrostatic patch coagulation (EPC) mechanism, Drying Technol. 28 (2010) 850–857.
[33] R.J. Haynes, M.S. Mokolobate, Amelioration of Al toxicity and P deficiency in acid soils by additions of organic residues: A critical review of the phenomenon and the mechanisms involved, Nutr. Cycling. Agroecosyst. 59 (2001) 47–63.
[34] J. Hur, M.A. Williams, M.A. Schlautman, Evaluating spectroscopic and chromatographic techniques to resolve dissolved organic matter via end member mixing analysis, Chemosphere 63 (2006) 387–402.
[35] T. Karanfil, M.A. Schlautman, I. Erdogan, Survey of DOC and UV measurement practices with implications for SUVA determination, J. Am. Water Works Assn. 94 (2002) 68–80.
[36] P.G. Coble, Characterization of marine and terrestrial DOM in seawater using excitation–emission matrix spectroscopy, Mar. Chem. 51 (1996) 325–346.
[37] T.F. Marhaba, D. Van, R.L. Lippincott, Rapid identification of dissolved organic matter fractions in water by spectral fluorescent signatures, Water Res. 34 (2000) 3543–3550.
[38] J. Bridgeman, A. Baker, C. Carliell-Marquet, E. Carstea, Determination of changes in wastewater quality through a treatment works using fluorescence spectroscopy, Environ. Technol. 34 (2013) 3069–3077.
[39] C.S. Uyguner, M. Bekbolet, Evaluation of humic acid photocatalytic degradation by UV–vis and fluorescence spectroscopy, Catal. Today 101 (2005) 267–274.
[40] J. Świetlik, E. Sikorska, Application of fluorescence spectroscopy in the studies of natural organic matter fractions reactivity with chlorine dioxide and ozone, Water Res. 38 (2004) 3791–3799.
[41] T. Zhang, J. Lu, J. Ma, Z. Qiang, Fluorescence spectroscopic characterization of DOM fractions isolated from a filtered river water after ozonation and catalytic ozonation, Chemosphere 71 (2008) 911–921.
[42] Y.Ş. Yıldız, A.S. Koparal, B. Keskinler, Effect of initial pH and supporting electrolyte on the treatment of water containing high concentration of humic substances by electrocoagulation, Chem. Eng. J. 138 (2008) 63–72.
[43] D. Ghernaout, M.W. Naceur, A. Aouabed, On the dependence of chlorine by-products generated species formation of the electrode material and applied charge during electrochemical water treatment, Desalination 270 (2011) 9–22.
[44] S. Van Geluwe, L. Braeken, B. Van der Bruggen, Ozone oxidation for the alleviation of membrane fouling by natural organic matter: A review, Water Res. 45 (12) (2011) 3551–3570.
[45] A.N. Pisarenko, D. Gerrity, E. Wert, B.D. Stanford, G. Korshin, S. Snyder, Use of Organic Characterization Techniques to Develop Predictive Tools for Water Reuse Applications, 15th annual Water Reuse & Desalination research conference, Las Vegas, NV, May 16–17, 2011.
[46] H. Zhang, Y. Zhang, Q. Shi, J. Hu, M. Chu, J. Yu, M. Yang, Study on transformation of natural organic matter in source water during chlorination and its chlorinated products using ultrahigh resolution mass spectrometry, Environ. Sci. Technol. 46 (2012) 4396–4402.
[47] C. Liu, V. Nanaboina, G. Korshin, Spectroscopic study of the degradation of antibiotics and the generation of representative EfOM oxidation products in ozonated wastewater, Chemosphere 86 (2012) 774–782.
[48] J. Chen, B. Gu, E.J. LeBoeuf, H. Pan, S. Dai, Spectroscopic characterization of the structural and functional properties of natural organic matter fractions, Chemosphere 48 (2002) 59–68.